ACS OMEGA

Article

Cite This: ACS Omega 2019, 4, 7850−7860

http://pubs.acs.org/journal/acsodf

Efficient Removal of Polycyclic Aromatic Hydrocarbons and Heavy Metals from Water by Electrospun Nanofibrous Polycyclodextrin Membranes

Asli Celebioglu,[†] Fuat Topuz,[†] Zehra Irem Yildiz,[†] and Tamer Uyar*[,†,‡]

[†]Institute of Materials Science & Nanotechnology, Bilkent University, Ankara 06800, Turkey

[‡]Department of Fiber Science & Apparel Design, College of Human Ecology, Cornell University, Ithaca, New York 14853, United States

Supporting Information

ABSTRACT: Here, a highly efficient membrane based on electrospun polycyclodextrin (poly-CD) nanofibers was prepared and exploited for the scavenging of various polycyclic aromatic hydrocarbons (PAHs) and heavy metals from water. The poly-CD nanofibers were produced by the electrospinning of CD molecules in the presence of a cross-linker (i.e., 1,2,3,4-butanetetracarboxylic acid), followed by heat treatment to obtain an insoluble poly-CD nanofibrous membrane. The membrane was used for the removal of several PAH compounds (i.e., acenaphthene, fluorene, fluoranthene, phenanthrene, and pyrene) and heavy metals (i.e., Pb^{2+}, Ni^{2+}, Mn^{2+}, Cd^{2+}, Zn^{2+}, and Cu^{2+}) from water over time. Experiments were made on the batch sorption of PAHs and heavy metals from contaminated water to explore the binding affinity of PAHs and heavy metals to the poly-CD membrane. The equilibrium sorption capacity (q_e) of the poly-CD nanofibrous membrane was found to be 0.43 ± 0.045 mg/g for PAHs and 4.54 ± 0.063 mg/g for heavy metals, and the sorption kinetics fitted well with the pseudo-second-order model for both types of pollutants. The membrane could be recycled after treatment with acetonitrile or a 2% nitric acid solution and reused up to four times with similar performance. Further, dead-end filtration experiments showed that the PAH removal efficiencies were as high as 92.6 ± 1.6 and 89.9 ± 4.8% in 40 s for the solutions of 400 and 600 μg/L PAHs, respectively. On the other hand, the removal efficiencies for heavy metals during the filtration were 94.3 ± 5.3 and 72.4 ± 23.4% for 10 and 50 mg/L solutions, respectively, suggesting rapid and efficient filtration of heavy metals and PAHs by the nanofibrous poly-CD membrane.

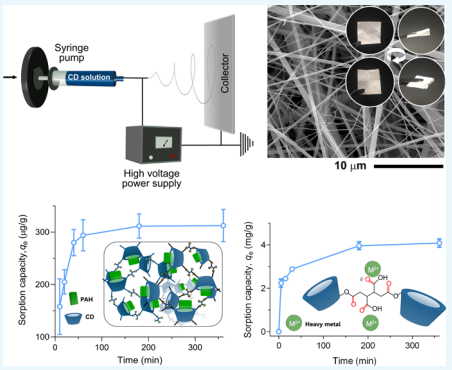

1. INTRODUCTION

Water is essential for sustaining life on earth and majorly polluted by municipal sewage discharges and industrial wastes.[1,2] Particularly, the latter one contains a wide spectrum of toxic substances, which can severely pollute clean water sources and pose a serious threat to the human health with their highly poisonous ingredients, for example, polycyclic aromatic hydrocarbons (PAHs).[3] PAHs constitute a major class of ubiquitous environmental organic micropollutants with fused aromatic groups, which are produced during the incomplete combustion of fossil fuels.[4] Because of their lipophilic nature, they are present in the soils of industrially contaminated sites at high concentrations[5] and with time, they pollute water sources and thus threaten human health.[6] Because of their poor water solubility (∼μg/L), they are present in water sources at ng/L concentrations.[7] Even such low levels of PAHs with consistent exposure may lead to accumulation in tissues[8] and thereafter can cause detrimental effects to the human health. In body, PAHs undergo metabolic activation by cytochrome P450 enzymes (principally, CYP1A1).[9] Furthermore, being lipophilic, they can cross cell membrane barriers and react with the cellular DNA,[10] forming PAH−DNA adducts as the first step of carcinogenesis.[11] Even though the body has their own protection control over the proofreading enzyme, DNA polymerase, to repair DNA damages, it sometimes cannot correct these errors during DNA replication. Thus, the U.S. Environmental Protection Agency (EPA) has fixed 16 PAH molecules as priority pollutants, including acenaphthene (Ace), fluorene (Flu), fluoranthene (FluA), phenanthrene (Phe), and pyrene (Pyr) and suggested a maximum allowable PAH concentration over benzo(*a*)pyrene (i.e., a carcinogenic PAH molecule) in drinking water as 200 ng/L.[12,13]

Similar to PAHs, heavy metals represent another important class of water pollutants, which are mostly discharged in industrial wastes and severely affect human health at concentrations above their acceptable limits. Above the critical concentrations, their presence can be life threatening for animals and humans. For instance, cadmium (Cd) is classified as a

Received: January 30, 2019
Accepted: April 17, 2019
Published: April 30, 2019

DOI: 10.1021/acsomega.9b00279
ACS Omega 2019, 4, 7850−7860

carcinogenic metal as many studies associated its presence with lung, prostate, and renal cancers in humans.[14] Furthermore, Cd mainly accumulates in the liver and kidney and thus induces kidney damage.[15] Likewise, lead (Pb) is a cumulative toxicant that can cause adverse health effects on body, particularly in children as the blood−brain barrier is less developed in children than adults, and Pb intake can thus induce serious brain damage in them.[15−17] Pb has also shown hematological and neurological effects in humans.[15] Another heavy metal nickel (Ni) is a widely used industrial precursor, and its presence at high levels can cause a serious threat to human health, including lung fibrosis, skin allergies, and cardiovascular system poisoning.[18] Likewise, the higher consumption of other heavy metals also gave rise to various health problems in human and animals, such as chronic copper (Cu) toxicity in sheep,[19] neutropenia and anemia because of very high zinc (Zn) consumption,[20] and nervous problems as a result of manganese (Mn) toxicity upon overexposure.[21]

Several sorbent materials have been developed to scavenge these toxic pollutants or minimize their presence in water sources, particularly in the sources of drinking water. Most strategies for PAH removal rely on the use of hydrophobic materials, which adsorb PAH molecules through interfacial adsorption. In this regard, Eeshwarasinghe et al. used a granular activated carbon (GAC) for the scavenging of PAH molecules from water whose removal by GAC took few hours.[22] Recent years have also witnessed to the development of specific removal systems for PAHs, of which removal occurs as intercalation, $\pi-\pi$, inclusion-complexation, and so forth. In this context, Topuz et al. described a bioinspired concept using DNA-based nanogels for the scavenging of PAH molecules from water.[23] Owing to the presence of a short diffusion pathway and interconnected matrix of DNA chains, rapid and efficient removal of PAHs was observed. Furthermore, for such systems, the removal process does not rely on interfacial adsorption, but on the complete swollen network. Langer and co-authors synthesized amphiphilic diblock copolymers for the preparation of photosensitive core−shell nanoparticles (NPs) for the removal of organic micropollutants, including PAHs.[24] Upon exposure to ultraviolet light, the colloidal stability of the NPs was significantly decreased by the removal of the protective layer and large aggregates were formed with the adsorbed pollutants. Another interesting strategy for PAH removal was developed by Stoddart group who synthesized a semi-rigid cyclophane with a shape of a box-like using 1,4-phenylene-bridged bipyridinium units.[25] The molecule was used for the removal of various PAH molecules, which formed inclusion-complexation with the cyclophane cavity. Likewise, cyclodextrin (CD)-functional materials were also used to remove PAHs from aqueous solutions through mostly host−guest inclusion complexation.[26,27] Recently, Dichtel and co-authors synthesized a porous β-CD polymer using tetrafluoroterephthalonitrile as a cross-linker for the scavenging of water micropollutants, including PAH derivatives, that is, 2-naphthol and 1-naphthyl amine, from water.[28] Because of the highly porous structure of the β-CD polymer and high affinity of CD molecules toward organic micropollutants, the β-CD-based polymeric material could rapidly scavenge organic micropollutants in few minutes. Similarly, various sorbents have been produced to get rid of heavy metals from water, including an eco-fabricated magnetic filter with mesh architectures composed of a soft magnetic material (Ni Zn) Fe_2O_4 and poly(acrylic acid) (PAAc)-coated quasi-superparamagnetic Fe_3O_4 NPs, which could decrease the concentrations of Pb^{2+} and Ni^{2+} from 1 to 0.01 mg/L for Pb^{2+} and 0.02 mg/L for Ni^{2+},[29] graphene oxide nanosheets with the maximum sorption capacities of 106.3 and 68.2 mg/g for Cd^{2+} and Co^{2+}, respectively,[30] polydopamine/bacterial nanocellulose membrane for highly efficient removal of Pb^{2+} and Cd^{2+},[31] and poly(amic acid) (PAA)-based vesicles for the removal of Ni^{2+} (from 58.7 to 0.095 ppm), Cu^{2+} (from 63.5 to 2.47 ppm), Zn^{2+}(from 65.4 to 0.58 ppm), and Pb^{2+} (from 207.2 to 0.87 ppm) in the presence of 1.0 mg/mL PAA vesicle.[32]

The production of CD-functional nanomaterials aimed at environmental applications has grown significantly in the last decade to snare various organic micropollutants, including PAHs, from water.[33−39] Particularly, CD-functional electrospun nanofibers have sparked great interest for the scavenging of PAHs because of their high surface to volume ratio and highly porous structure for enhanced sorption performance. In this regard, we previously reported CD-grafted cellulose acetate nanofibers for PAH scavenging.[40] The incorporation of CD molecules via click reaction enhanced the sorption performance of cellulose acetate nanofibers. Likewise, CD-decorated polyester nanofibers were prepared by the post-modification of polyester nanofibers with CD using citric acid (CA) as a coupler.[41] CD functionalization improved the PAH-removal performance of pure polyester nanofibers. Recently, we developed a high-performance, water-insoluble nanofibrous poly-CD membrane cross-linked by a carboxylic acid-based cross-linker for the sequestration of methylene blue (MB) dye.[42] Because such nanofibers were only composed of CD and cross-linker, they showed very high sorption performance in the scavenging of MB from aqueous solutions. Likewise, an insoluble poly-CD fibrous mat was produced by cross-linking with epichlorohydrin as a highly efficient sorbent material for the removal of phenanthrene.[43] CD-functional nanofibers were also used for the removal of heavy metals from aqueous solutions. In one example, nonwoven poly(ethylene terephthalate) (PET) coated with β-CD-polycarboxylic molecules [i.e., CA, 1,2,3,4-butanetetracarboxylic acid (BTCA) and poly(acrylic acid)] was used for the removal of four heavy metals (i.e., Pb^{2+}, Cd^{2+}, Zn^{2+}, and Ni^{2+}) from water.[44] Depending on the type of carboxylic component, the materials showed different removal performance. The highest removal capacity was observed when BTCA was used for CD decoration. Thus, the presence of carboxylic groups in CD fibers allows their use for the removal of heavy metals, whereas accessible CD cavities can make host−guest inclusion complexation with PAH molecules.

In this study, electrospun CD nanofibers were prepared by the electrospinning of hydroxypropyl β-CD (HP-β-CD) molecules in the presence of a tetracarboxylic acid-functional cross-linker and sodium hypophosphite as an initiator. The cross-linking of the CD nanofibers led to an insoluble, hydrophilic nanofibrous poly-CD membrane, which was used for the scavenging of several PAHs (i.e., Ace, Flu, FluA, Phe, and Pyr) and heavy metals (i.e., Pb^{2+}, Ni^{2+} Mn^{2+}, Cd^{2+}, Zn^{2+}, and Cu^{2+}) from water over time. The sorption performance of the PAHs was explored over batch sorption experiments by the gas chromatography−mass spectrometry (GC−MS) analysis, whereas inductively coupled plasma (ICP)-MS was used to monitor the removal of the heavy metals by the poly-CD membrane. Furthermore, the filtration performance of the membrane for both types of pollutants was tested through a dead-end filtration system, and the stability of nanofibers after the filtration was explored over morphological analysis by scanning electron microscopy (SEM).

DOI: 10.1021/acsomega.9b00279
ACS Omega 2019, 4, 7850−7860

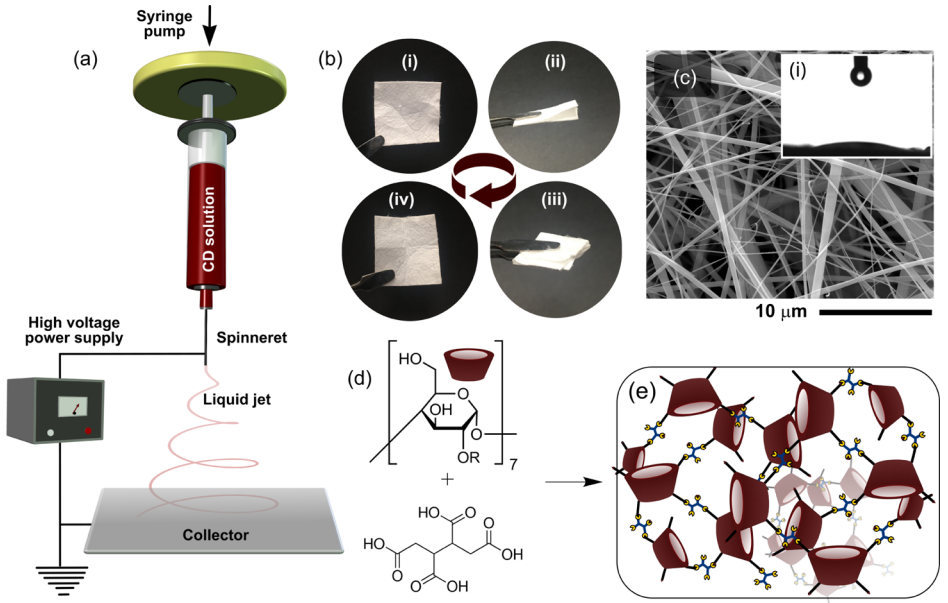

Figure 1. Production of the nanofibrous poly-CD membrane. (a) Electrospinning of an aqueous solution of the HP-β-CD. (b) Photos of the membrane during the folding process. (c) Scanning electron micrograph of the membrane. The inset (i) shows the wettability of the membrane surface. (d) Chemical reaction between BTCA and CD molecules, and (e) representative cartoon illustration of the poly-CD network in the membrane.

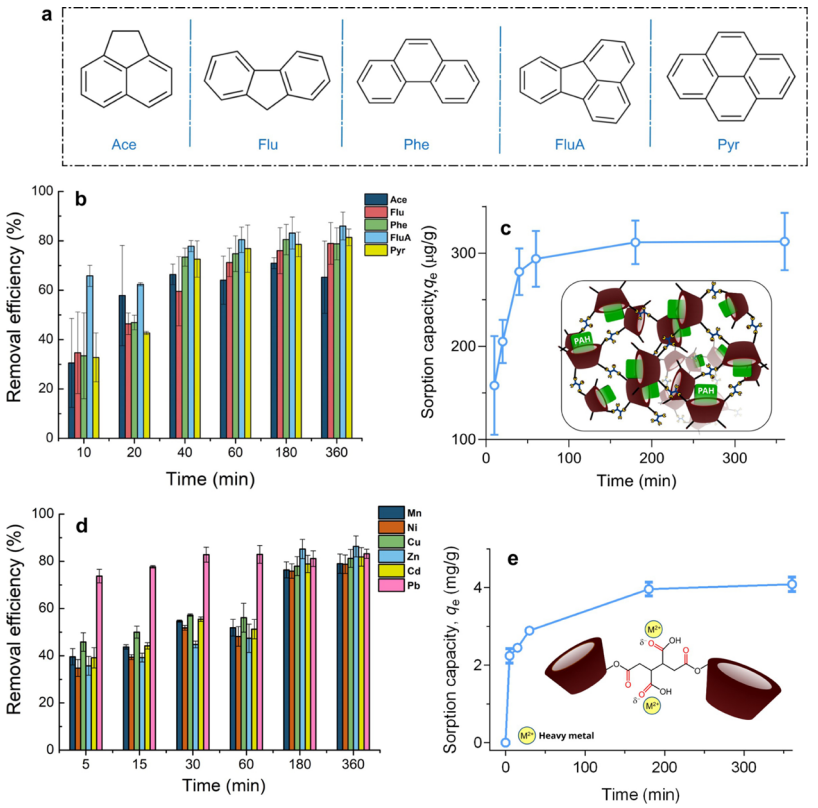

Figure 2. (a) Chemical structures of the PAHs used in the sorption experiments. (b) Removal efficiency of the PAHs over time using the poly-CD membrane. The initial PAH concentration was 400 μg/L. (c) Adsorption capacity (q_e) during the removal of PAHs. The inset (c) shows a cartoon illustration of inclusion-complex formation between PAH and CD in the fiber matrix. (d) Removal efficiency of the heavy metals over time using the poly-CD membrane. The initial concentration of heavy metals was 5 mg/L. (e) Sorption capacity (q_e) during the removal of heavy metals. The inset (e) displays the possible electrostatic interaction between carboxyl group and heavy metal.

DOI: 10.1021/acsomega.9b00279
ACS Omega 2019, 4, 7850−7860

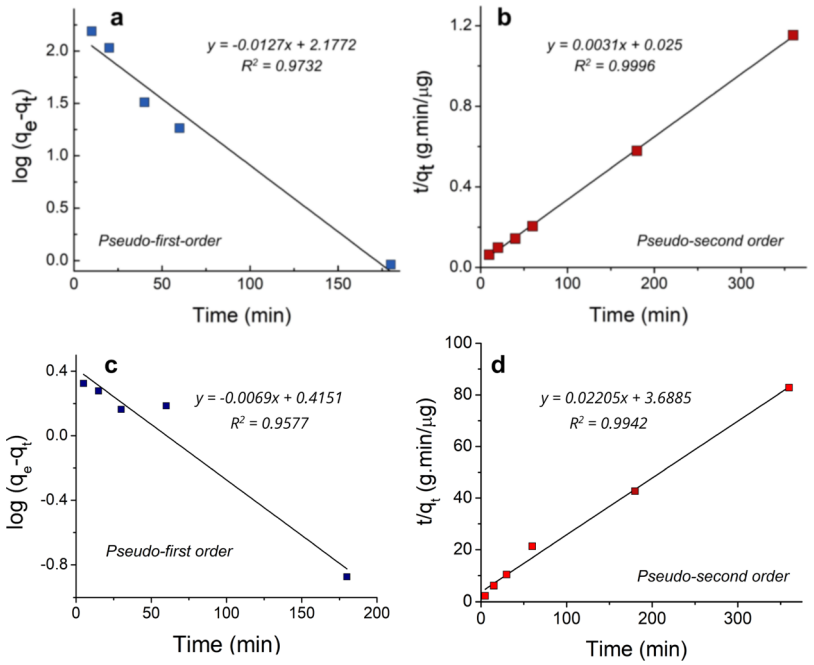

Figure 3. (a) Pseudo-first-order kinetic and (b) pseudo-second-order kinetic plots for PAH removal from water. The PAH concentration was 400 μg/L. (c) Pseudo-first-order kinetic and (d) pseudo-second-order kinetic plots for heavy metal removal from water. The concentration of heavy metals was 5 mg/L.

2. RESULTS AND DISCUSSION

2.1. Preparation of the Poly-CD Nanofibrous Membrane by Electrospinning. The nanofibrous CD membrane was prepared by the electrospinning of aqueous solutions of HP-β-CD molecules in the presence of the cross-linker and initiator, following our previous method (Figure 1a).[42] After an appropriate time of electrospinning, a nanofibrous CD mat with a suitable thickness/size was produced. The mat was cross-linked with heat treatment at 175 °C for 1 h, which led to the formation of a nanofibrous poly-CD membrane (Figure 1b). The resultant membrane was a self-standing and handy material and could be folded without any structural damage, demonstrating its suitability for sorption applications. Figure 1c shows the SEM image of the nanofibers and the water wettability of the membrane surface. The mean fiber diameter was calculated as 480 ± 300 nm for the nanofibrous poly-CD membrane (Figure 1c). Owing to the hydrophilic nature of the poly-CD membrane, the water droplet spreads across the membrane surface [Figure 1c (inset)]. This can be attributed to the hydrophilic nature of both components (HP-β-CD and BTCA) in the resultant cross-linked network (Figure 1d,e). The cross-linking of the HP-β-CD molecules by BTCA was confirmed by the XPS analysis. Figure S1 shows the deconvoluted C 1s XPS spectra of the HP-β-CD mat and poly-CD membrane. The deconvoluted C 1s XPS spectra of the poly-CD membrane show a peak related to O−C═O of the reacted and unreacted carboxyl groups as well as the formed ester bonds at 289.10 eV. On the other hand, this peak is not visible for the HP-β-CD fibers. Furthermore, the ratio of C−C and C−H bonds (appeared at 284.85 eV) significantly increases from 29.93 to 37.56% after cross-linking. The reaction between carboxylic acid and hydroxyl group produces H_2O as a by-product, which decreases O content in the overall composition (Table S1). The cross-linking of the nanofibers did not show any significant change on the XRD pattern of the HP-β-CD mat, whereas the electrospinning of HP-β-CD nanofibers increased the amorphous structure of HP-β-CD molecules because of their random organization during the electrospinning process (Figure S2). The intensities of broad peaks of HP-β-CD molecules centered at 18.84 (d-spacing: 4.67 Å) and 10.55° (d-spacing: 8.55 Å) significantly decreased after the electrospinning process (Figure S2).

2.2. Adsorption Kinetics. The poly-CD membrane was used for the removal of several PAH compounds (i.e., Phe, FluA, Ace, Flu, and Pyr) from water (Figure 2a). During the sorption experiments, the membrane was treated with the mixed solutions of five different PAHs over time to explore the sorption kinetics as well as their affinity to form inclusion complexes with functional CD molecules. The aqueous solubility order of the respective PAH molecules is as follows: Ace (1.93 mg·L^{-1}) ≥ Flu (1.90 mg·L^{-1}) > Phe (1.20 mg·L^{-1}) ≫ FluA (0.26 mg·L^{-1}) ≫ Pyr (0.077 mg·L^{-1}) > Ant (0.076 mg·L^{-1}).[45] The initial concentration of the PAH solution was kept at 400 μg/L (i.e., the concentration of each PAH was 80 μg/L in the respective mixture), which decreased significantly over time due to the formation of inclusion complexes with active CD molecules and the adsorption of PAHs on hydrophobic domains in the poly-CD fibrous network. On the course of the PAH treatment, samples were taken from PAH solutions at certain intervals and measured by GC−MS. Figure 2b shows the PAH-sorption performance of the membrane as a function of time. The removal efficiency showed variations for each PAH molecule because of differences in the binding affinity of the PAHs to the CD cavity. Even after 10 min, the PAH content decreased over 30% for all PAHs tested, demonstrating the presence of high-functional CD content in the membrane. The highest removal efficiency was observed for fluoranthene (FluA) with a significant concentration decrease (i.e., over 60%). This may be attributed to the high affinity of HP-β-CD molecules toward FluA. A similar finding was reported by our previous study, where we observed the highest sorption capacity for FluA when poly-CD cryogels were used as sorbent materials.[26] After

DOI: 10.1021/acsomega.9b00279
ACS Omega 2019, 4, 7850−7860

Table 1. Kinetics Parameters for the Sorption of PAHs and Heavy Metals by the Poly-CD Membrane

	experimental	pseudo-first order model			pseudo-second order model		
	q_{exp} (mg/g)	q_e (mg/g)	k_1 (min^{-1})	R^2	q_e (mg/g)	k_2 ($g \cdot mg^{-1}\ min^{-1}$)	R^2
PAHs	0.312 (±0.030)	0.150	0.0055	0.973	0.320	3.9×10^{-4}	0.9996
heavy metals	4.351 (±0.078)	2.600	0.0029	0.957	4.536	1.3×10^{-2}	0.9942

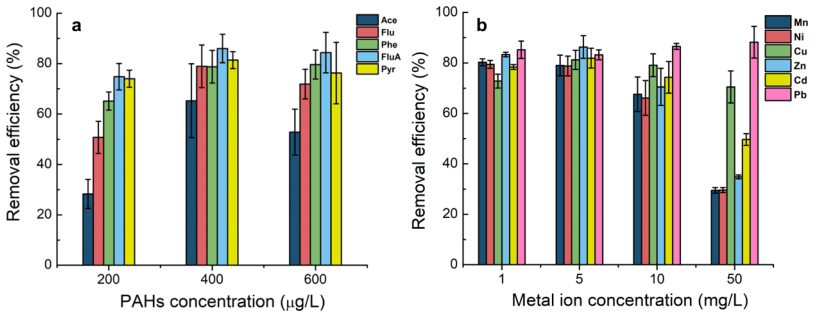

Figure 4. Equilibrium removal efficiency (%) of (a) PAHs and (b) heavy metals by the poly-CD membrane at various concentrations of pollutants.

20 min, the removal efficiency reached 50%, suggesting rapid scavenging of PAHs by the poly-CD membrane due to the presence of functional CD molecules (i.e., CD molecules that can make host−guest complexation) (Figure 2c) and unspecific adsorption of PAHs on hydrophobic domains in the poly-CD fibrous matrix. The equilibrium sorption was observed after 60 min, whereas no significant increase in the sorption was observed up to 360 min, suggesting that the system reached saturation, and at this point, the mean removal capacity of the five PAHs was found to be 78.1 ± 7.7%. The affinity of the poly-CD membrane toward PAHs was found in an order of FluA > Pyr > Phe > Flu > Ace. The lowest removal efficiency was observed for acenaphthene (Ace) among the PAHs tested. In this regard, Morillo et al. reported the enhanced solubilization of various PAHs by different synthetic CDs [HP-β-CD, HP-γ-CD, and randomly methylated (RM) β-CD] for remediation applications.[45] They observed that the binding constant (K_c) of PAHs with HP-β-CD follows the following order: Phe > FluA > Flu > Pyr > Ace. The lowest K_c was observed for Ace, which is in agreement with our sorption finding. After 3 h treatment, the lowest removal efficiency was observed for Ace by the nanofibrous poly-CD membrane (Figure 2b). On the other hand, the highest removal was observed for FluA after 3 h, followed by Phe, whereas they observed the highest binding affinity for Phe when they use HP-β-CD molecules. In this study, we use poly(HP-β-CD) networks for the removal of PAHs. The cross-linking of HP-β-CD molecules can change the cavity size of the CD molecules. In this regard, it was reported that the methylation of β-CD increases the cavity volume by 10−20% as a result of enhanced depth of the cavity up to 10−11 Å;[46] therefore, RM β-CD showed higher solubility of PAHs than HP-β-CD.[45] Given that the possible enhanced cavity volume because of cross-linking, the poly-HP-β-CD, unlike HP-β-CD, can show different binding affinities for PAH molecules. In addition to inclusion-complexation with functional CD molecules, unspecific adsorption of PAHs on the hydrophobic domains takes place, which may change the sorption capacity for a specific PAH molecule. The poly-CD membrane was also used for the removal of six different heavy metals (i.e., Pb^{2+}, Ni^{2+}, Mn^{2+}, Cd^{2+}, Zn^{2+}, and Cu^{2+}) from water. The removal efficiencies of heavy metals as a function of time are shown in Figure 2d. About 40% removal was observed after 5 min treatment, suggesting rapid and efficient removal of heavy metals by the poly-CD membrane. Interestingly, at that time, the removal efficiency for Pb was higher than 70% because of very high affinity of Pb toward the unreacted carboxyl groups and the oxygen of carbonyl groups (the polarity of the C═O bond induces a partial negative charge on the oxygen group). After 6 h treatment, the adsorption reached to equilibrium (Figure 2e).

The sorption kinetics gives an assessment regarding equilibrium sorption time and capacity as well as insights into kinetics mechanism. The sorption mechanism of PAHs and heavy metals was explored by plotting the sorption kinetics according to the pseudo-first- and pseudo-second-order models (Figure 3). The respective kinetics parameters are given in Table 1. R^2 values were found as 0.9732 and 0.9577 according to the pseudo-first-order kinetic model (Figure 3a,c). However, a better fit was observed for the pseudo-second-order kinetic model with R^2 of 0.9996 and 0.9942 for PAHs and heavy metals, respectively (Figure 3b,d). According to the pseudo-second-order model, the equilibrium adsorption capacities (q_e) were calculated as 0.31 ± 0.030 and 4.54 ± 0.063 mg/g for PAHs and heavy metals, respectively, which are in line with the experimental findings (q_{exp}, Table 1). A similar kinetic model was observed for the β-CD-grafted activated carbon during the adsorption of the simplest PAH molecule, naphthalene.[47] Because the sorption of PAHs onto CDs mainly takes place as through clathration and hydrophobic interactions, the inclusion process was influenced greatly by the shape, size, and polarity of the guest PAH molecule. Thus, the rate constant k_2 value for PAHs is controlled by the clathration.

The PAH-removal process can be explained by the formation of inclusion complexes between CD and PAHs as well as adsorption of PAHs onto hydrophobic domains in the poly-CD fibrous matrix. Figure 4a shows the PAH-removal efficiency from aqueous solutions using the poly-CD membrane in the presence of various PAH concentrations (i.e., 200, 400, and 600 μg/L). The PAH-removal performance increased proportionally with respect to the PAH content. Even at the PAH concentration of 600 μg/L, the mean removal efficiency of the membrane was above 80%, suggesting the efficient scavenging of the PAHs. The equilibrium sorption capacity was found as 0.43 ± 0.045 mg/g material when the PAH concentration was 600 μg/L. For all concentrations, the highest removal was observed for FluA, followed by Pyr, whereas the lowest removal was observed for Ace. Differences in the removal efficiencies can be

DOI: 10.1021/acsomega.9b00279
ACS Omega 2019, 4, 7850−7860

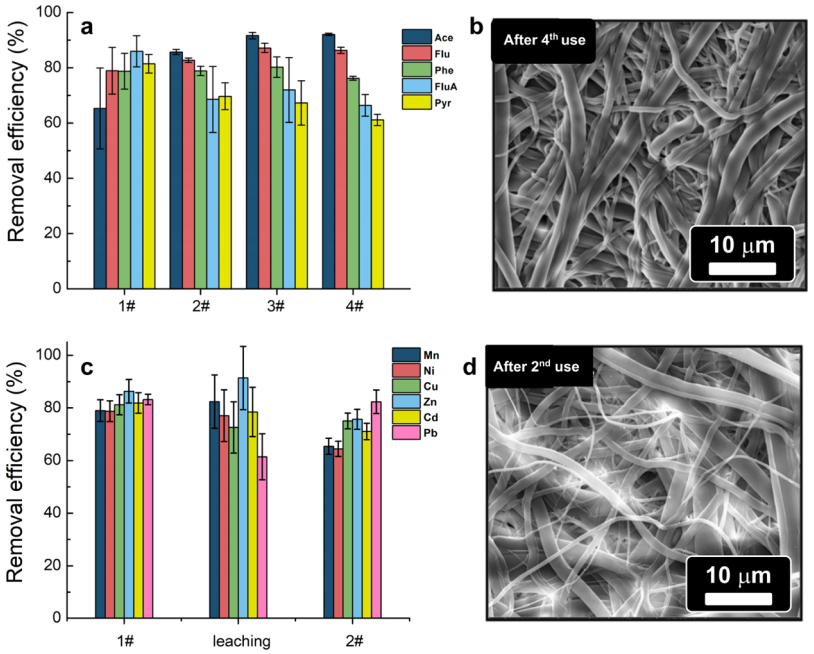

Figure 5. Reusability of the nanofibrous poly-CD membrane for the sorption of (a) PAHs and (c) heavy metals. After each cycle, the membrane was washed with acetonitrile (for PAHs) or 2% nitric acid solution (for heavy metals). Scanning electron micrographs of the nanofibrous poly-CD membrane after (b) 4th use for PAH removal and (d) 2nd use for heavy metal sorption.

ascribed to the binding affinity of CD molecules toward the respective PAH. On the other hand, the removal of heavy metals mainly takes place electrostatically over carboxylic and carbonyl groups. The poly-CD membrane was used for the scavenging of heavy metals of various concentrations (1, 5, 10, and 50 mg/L) (Figure 4b). For three concentrations (1, 5, and 10 mg/L), the membrane showed identical removal efficiency, whereas a significant decrease in the removal efficiency was observed with increasing the heavy metals concentration to 50 mg/L. However, even at this concentration, the removal efficiency for Pb ions was 90%, demonstrating the high affinity of Pb ions to the membrane.

The reusability of the membranes is highly critical by the reason of monetary and environmental issues. In this regard, the nanofibrous poly-CD membrane is a handy material and could be separated from the adsorbed PAHs and heavy metals through a simple washing with acetonitrile or a 2% nitric acid solution, respectively. The reusability of the membrane was explored up to four times, and after each use, the removal of the adsorbed PAHs from the membrane was carried out by washing the membrane with acetonitrile. During repetitive use, the removal efficiency for PAHs was found between 70 and 80% after each use, demonstrating their reusability (Figure 5). Likewise, the reusability of the membrane for heavy metal scavenging was explored. In this case, the leached metals could also be measured after the treatment with 2% nitric acid. Thereafter, the reuse of the membrane for heavy metal removal showed a small loss in the sorption performance. This can be attributed to that not all bound heavy metal ions are leached from the fiber matrix so that the removal efficiency slightly decreased. After repetitive use, the morphology of the poly-CD membrane was explored by SEM (Figure 5b,d), where fibers were swollen to some extent, but the fibrous structure of the membrane was maintained.

2.3. Filtration Performance of the Poly-CD Membrane.

Although the fibrous structure of the poly-CD membrane was maintained, fibers were swollen because of water diffusion in the hydrophilic matrix of the poly-CD during their use in aqueous solutions. Increasing cross-linker concentration or incubation temperature during the fabrication of the membrane can lead to more stable poly-CD nanofibers. Owing to its structural stability during the sorption tests, the filtration performance of the membrane for both PAHs and heavy metals was explored using a dead-end filtration system. In the filtration tests, the membrane

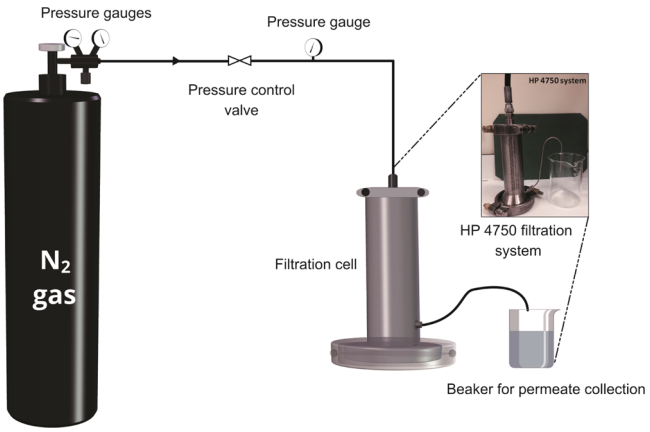

Figure 6. Cartoon illustration of a dead-end filtration system. The membrane inserted in the high-pressure Sterlitech HP4750 cell, and the pollutant solution (50 mL) was added and passed through the membrane with an active filtration of 14.6 cm^2 under N_2 pressure (10^4 Pa). The filtered solution was collected in a beaker.

was transferred into a high-pressure cell [HP4750 (Sterlitech)] and 50 mL of PAH solutions (having concentrations of 400 and 600 μg/L) or 50 mL of heavy metals (having concentrations of 10 and 50 mg/L) passed through the membrane with an active filtration area of 14.6 cm^2 under a certain N_2 pressure at 10^4 Pa (Figure 6). This pressure was reported to be an optimum pressure for the poly-CD membrane according to our previous

DOI: 10.1021/acsomega.9b00279
ACS Omega 2019, 4, 7850−7860

Table 2. Conditions of the Dead-End Filtration System[a]

pollutant (concentration)	permeability (P_w) (L m^{-2} h^{-1} kPa^{-1})	flux (F) (L m^{-2} h^{-1})	removal efficiency (%)
PAH (400 μg/L)	237 ± 80	3090 ± 500	92.6 ± 1.6
PAH (600 μg/L)	242 ± 12	3302 ± 50	89.9 ± 4.8
M^{2+} (10 mg/L)	245 ± 70	3358 ± 365	94.3 ± 5.3
M^{2+} (50 mg/L)	236 ± 14	3310 ± 197	72.4 ± 23.4

[a]The removal efficiency (%) of PAHs by the nanofibrous poly-CD membrane after filtration tests.

study for the filtration of MB.[42] The removal efficiencies for PAHs were calculated as 92.6 ± 1.6 and 89.9 ± 4.8% for the solutions containing 400 and 600 μg/L PAHs, respectively (Table 2). These results are in line with the sorption values obtained at the equilibrium. For heavy metals, the removal efficiencies were calculated as 94.3 ± 5.3 and 72.4 ± 23.4% for 10 and 50 mg/L solutions, respectively. Even though the filtration experiments were performed in 40 s for 50 mL stock solutions, this high performance can be attributed to the presence of functional CD molecules and as well unspecific adsorption of PAHs on the hydrophobic segments in the poly-CD fibrous matrix. Furthermore, XPS analysis was performed on the membranes used for the filtration of heavy metals of two different concentrations (10 and 50 mg/L) (Figure S3). The most prominent intensities were observed for Pb^{2+}, Cu^{2+}, and Cd^{2+}, demonstrating higher adsorption of these metal ions by the poly-CD membrane. In general, the intensity levels were nearly correlated with the removal efficiency values of metal ions (Figure 4b). Additionally, the intensity belonging to respective metals increased distinctively as the concentration increased from 10 to 50 mg/L, demonstrating the higher adsorbed amount of heavy metals onto the poly-CD membrane (Figure 4b). The presence of carboxyl and carbonyl groups enhanced the sorption performance for heavy metals, and the nanofibrous poly-CD membrane could rapidly scavenge metal ions from water.

Furthermore, the flux (F) and permeability (P_w) are two significant factors that determine the filtration performance of membranes. The respective values for the nanofibrous poly-CD membrane were calculated as 237 ± 80 L m^{-2} h^{-1} kPa^{-1} and 3090 ± 500 L m^{-2} h^{-1} for PAHs, whereas they were calculated as 245 ± 70 L m^{-2} h^{-1} kPa^{-1} and 3358 ± 365 L m^{-2} h^{-1} for heavy metals, respectively (Table 2). Furthermore, no flux fluctuation was observed during filtration, and the process was completed with a stable permeation flux. These values are much higher than most of the electrospun membranes used for water depollution and desalination. In one example, Obaid et al. produced membranes based on amorphous silica NP-incorporated poly(vinylidene fluoride) electrospun nanofiber mats for water desalination.[48] The membrane showed water flux of 83 L m^{-2} h^{-1} and salt rejection of 99.7% for 2 M NaCl draw solution. Dobosz et al. used electrospun nanofibers of cellulose or polysulfone with ultrafiltration membranes for the removal of poly(ethylene glycol) (PEG) molecules of various molecular weights.[49] The membranes showed very high water flux (~1200 L m^{-2} h^{-1}) at the pressure of 1.5 bar. Even though in the presence of such high pressure, this water flux is lower than the nanofibrous poly-CD membrane, which has flux over 3000 L m^{-2} h^{-1} at 10 kPa (0.1 bar) (Table 2). Rejection was found to be related to the molecular weight of PEGs, and the membranes showed selective rejection to higher molecular weights of PEGs (M_w > 150 kDa) with rejection over 80%. Coelho et al. produced membranes from electrospun poly(vinyl alcohol) and poly(catechol) nanofibers on a poly(vinylidene fluoride) basal disc for the filtration of reactive Red 66 monoazo dye from distilled water and seawater.[50] The membranes showed an average flux rate of 70 L m^{-2} h^{-1} for distilled water and 62 L m^{-2} h^{-1} for seawater at 4 bar. The respective rejection rates were found to be 85 and 64% for distilled water and seawater. Dong et al. produced superhydrophobic membranes based on fluoroalkylsilane-grafted PVA nanofibers.[51] The membranes showed high permeate flux of 25.2 kg m^{-2} h^{-1} and have potential for their use in water desalination. An interesting nanofibrous membrane was developed by Chu and co-workers by incorporating cellulose nanowhiskers into electrospun PAN and PET nonwoven substrates.[52] The incorporation of cellulose nanowhiskers significantly enhanced the adsorption capacity of the membrane by 16 times. The PAN electrospun membrane showed water flux of 83 L m^{-2} h^{-1} kPa^{-1}, whereas cellulose nanowhiskers incorporated electrospun membrane showed water flux of 59 L m^{-2} h^{-1} kPa^{-1} which is much lower than the nanofibrous poly-CD membrane. Overall, the poly-CD membrane has very high permeability and water flux and is superior to most of the electrospun membrane reported in the literature.

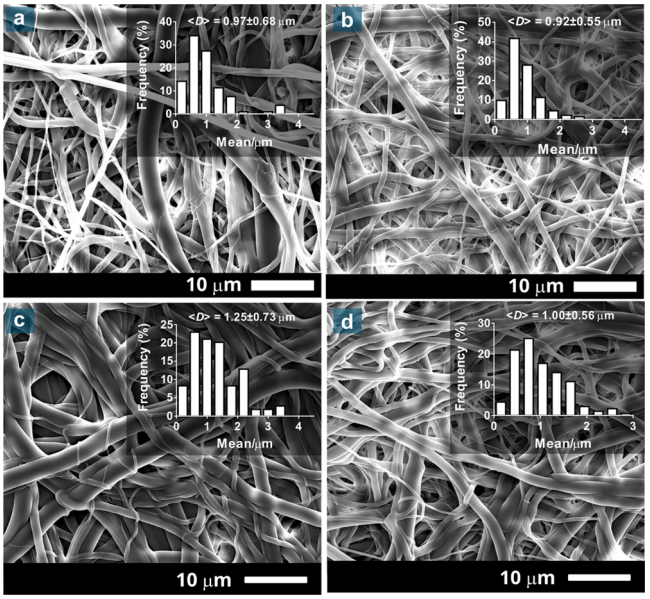

Figure 7. Scanning electron micrographs of the nanofibrous poly-CD membrane after its use in the filtration test for PAHs of concentrations of (a) 400 and (b) 600 μg/L and heavy metals of concentrations of (c) 10 and (d) 50 mg/L. Insets show the size distribution plots of the respective fibers.

2.4. Stability of the Poly-CD Membrane. The morphology of the poly-CD membrane after its use several times is shown in Figure 5b,d where the samples maintained their fibrous structure, suggesting the structural stability of the membrane due to efficient cross-linking reactions between CD and BTCA. The morphology of the nanofibers was also explored after the filtration tests (Figure 7). Figure 7a,b shows the SEM photos of the poly-CD membranes after their use in the filtration of PAHs at two different concentrations (400 and 600 μg/L). For both cases, the fibrous structure of the poly-CD membrane was maintained, but the swelling of nanofibers was observed: the mean fiber diameter increased from 400 ± 350 to 970 ± 680 and

DOI: 10.1021/acsomega.9b00279
ACS Omega 2019, 4, 7850−7860

920 ± 550 nm after treatment with 400 and 600 μg/L PAH solutions, respectively. A similar trend was observed for the poly-CD nanofibers treated with heavy metals at two different concentrations (10 and 50 mg/L): the mean diameter of the fibers increased to 1250 ± 730 and 1000 ± 560 nm, respectively. The preservation of the nanofibrous structure of the poly-CD membrane after filtration tests suggests the structural stability of the poly-CD nanofibers because of their highly cross-linked structure. Owing to the hydrophilic nature of components, nanofibers in the poly-CD membrane were swollen to some extent while maintaining the fibrous structure. This could be attributed to the presence of efficient cross-linking between the HP-β-CD and BTCA. Nevertheless, a more robust nanofibrous poly-CD membrane can be fabricated by tuning of cross-linking efficiency and cross-linking density over process parameters and concentrations of precursors.

3. CONCLUSIONS

The nanofibrous poly-CD membrane was produced and exploited for the scavenging of several PAH molecules and heavy metals from water. The SEM analysis of the poly-CD membrane revealed the bead-free fiber structure, which could maintain its nanofibrous structure in water because of the densely cross-linked CD network structure. The nanofibrous poly-CD membrane successfully removed several PAHs (i.e., Flu, Ace, Pyr, Phe, and FluA) and heavy metals (i.e., Pb^{2+}, Ni^{2+}, Mn^{2+}, Cd^{2+}, Zn^{2+}, and Cu^{2+}) from water with the equilibrium sorption capacities of 0.43 ± 0.045 and 4.54 ± 0.063 mg/g for PAHs and heavy metals, respectively. The sorption took place according to the pseudo-second-order kinetic model and reached to equilibrium in 60 min, whereas the membrane could reduce PAH and heavy metal content by half in 20 min, suggesting rapid and efficient removal of the PAHs and heavy metals from water. Furthermore, during the filtration, the poly-CD membrane could rapidly reduce the PAH content by ca. 90% in 40 s when the solutions with PAH concentrations of 400 and 600 μg/L were used. A similar performance was observed during the filtration of heavy metals. The SEM analyses of the nanofibrous poly-CD membrane after the filtration and sorption tests revealed that the fiber morphology was maintained to some extent. Because of the nanofibrous and handy structure, the poly-CD membrane is a suitable sorbent material for the removal of PAHs or heavy metals from water.

4. EXPERIMENTAL SECTION

4.1. Materials. HP-β-CD with a molar substitution between 0.6 and 0.9 was kindly received as a gift from Wacker Chemie AG (Germany). Sodium hypophosphite hydrate (SHP, Sigma-Aldrich), BTCA (Sigma-Aldrich, 99%), PAHs [acenaphthene (Ace, 99%), fluorene (Flu, 98%), fluoranthene (FluA, 98%), phenanthrene (Phe, 98%), and pyrene (Pyr, 98%)], and heavy metals (zinc(II) acetate, manganese(II) acetate, lead(IV) acetate, cadmium(II) acetate, copper(II) acetate, and nickel(II) acetate) were all obtained from Sigma-Aldrich. High-purity water was produced from a Millipore Milli-Q system (resistivity ≥ 18 MΩ cm).

4.2. Production of the Poly-CD Nanofibrous Membrane by Electrospinning. The nanofibrous poly-CD membrane was produced according to our previous method.[42] Briefly, HP-β-CD with a concentration of 140% (w/v) was dissolved in water, and afterward, the cross-linker (BTCA, 20 wt % according to the CD content) and initiator (SHP, 2% according to the CD content) were added. The solution was held at 50 °C under continuous stirring for few minutes. Thereafter, the solution cooled down to room temperature and transferred into a syringe having a metallic needle of an inner diameter of 0.45 mm. The syringe put on horizontally in a KDS-101 model syringe pump (KD Scientific), and a high voltage power (Matsusada Precision, AU Series) was applied. The nanofibers were collected on a metal collector covered with an aluminum foil. During the electrospinning, the following parameters were used: the applied voltage of 10 kV, the flow rate of 1 mL/h, and a tip-to-collector distance of 10 cm. The electrospinning was performed at 24 °C in the presence of 25−30% relative humidity. The nanofiber mat put in an oven and kept at 175 °C for 1 h for the cross-linking reactions and, thereafter, treated with water and ethanol/acetonitrile to remove unreacted precursors. A pristine nanofibrous HP-β-CD mat without using BTCA and SHP was also prepared to explore the influence of cross-linking process on the morphology of HP-β-CD fibers by SEM and phase identification of HP-β-CD molecules over XRD analysis. The electrospinning of HP-β-CD at 160% (w/v) from aqueous solution resulted in a HP-β-CD nanofibrous mat. The electrospinning parameters for HP-β-CD nanofibers were as follows: tip-to-collector distance was 15 cm, the flow rate set to 0.5 mL/h, and the applied voltage was 15 kV.

4.3. Scanning Electron Microscopy. The fiber morphology was explored by SEM (Quanta 200 FEG, FEI). The fiber specimens were coated with 5 nm Au/Pd with a PECS-682 sputter. The mean fiber diameter was determined from the SEM images over 100 nanofibers by ImageJ software (NIH, US National Institutes of Health).

4.4. Sorption Tests. *4.4.1. PAH-Sorption Tests.* The scavenging of PAH molecules was monitored using a GC−MS (model 7890A) coupled to a 5975C inert MSD with a Triple-Axis detector (Agilent Technologies). Before the loading of the filtered solutions to the detection system, PAH molecules were separated from an aqueous environment to hexane by a liquid−liquid extraction. Afterward, the hexane solution (1 μL) was injected to GC−MS by an injector (MSU 011-00A, volume = 10 mL, scale = 54 mm). An HP-5MS (Hewlett-Packard, Avondale, PA) capillary column (30 m × 0.25 mm ID, 0.25 μm film thickness) could separate compounds. The temperature of the column was maintained at 80 °C for 2 min and increased to 250 °C with a rate of 10 °C/min and then equilibrated at this temperature for 2 min. A carrier gas (He) with a flow rate of 1.2 mL/min was exploited. The splitless mode was used for the thermal desorption. The temperature of the transfer line and ion source was kept at 290 and 230 °C, respectively. A complete scanning mode (SCAN) was used to determine all PAH peaks. During the measurements, the selected ion monitoring was implemented. The retention time of Ace, Flu, FluA, Phe, and Pyr was 11.09, 12.27, 17.33, 14.51, and 17.84 min, and the major peaks of the PAHs were 153.1, 166.1, 202.1, 178.1, and 202.1 mass over charge, respectively. The results were adapted to calibration curves, which were obtained for the PAH concentrations of 200−600 μg/L with $R^2 \geq 0.99$ linearity and acceptability over the peak areas under curves. The adsorption of PAHs on different glass containers was also explored, and the partial adsorption of the PAHs on the glass surface was observed to some extent (Figure S4). The lowest adsorption was observed for GC−MS vials that were used for sorption experiments.

4.4.2. Heavy Metal Sorption Tests. A Thermo-X series II inductively coupled plasma-mass spectrometer was used to measure heavy metal concentrations during the removal

DOI: 10.1021/acsomega.9b00279
ACS Omega 2019, 4, 7850−7860

experiments. To prevent the precipitation of metal ions, test solutions were diluted with 2% nitric acid solution. The calibration curve was made of five different concentrations of standard metal ion solutions (25−1000 μg/L) with the $R^2 \geq 0.99$ acceptability. The ICP-MS operating parameters were dwell time: 10 000 ms, channel per mass: 1, acquisition duration: 7380, channel spacing: 0.02, and carrier gas: argon.

4.5. Batch Sorption Experiments. Batch adsorption experiments were carried out by shaking at 160 rpm on a magnetic stirrer (IKA-KS 130, Germany). The stock solutions of PAHs were prepared from the mixture of PAHs, that is, Ace, Flu, FluA, Phe, and Pyr. The analysis of batch adsorption tests was performed by using GC−MS. On the other hand, for heavy metal removal experiments, 5 mg of adsorbent and 5 mL of metal ion solutions consisted of Pb^{2+}, Ni^{2+}, Mn^{2+}, Cd^{2+}, Zn^{2+}, and Cu^{2+} were used. Kinetic experiments were performed under the conditions of 5 mg/L concentrated heavy metal ion solution.

Because of the poor water solubility of the PAHs, the experiments were performed according to their solubility limits in water. In this regard, 200, 400, and 600 μg/L concentrated solutions were prepared and used in the removal tests. Poly-CD membranes (~5 mg) were immersed in 5 mL of 400 μg/L PAH solution (i.e., 80 μg/L of each in the resultant mixture) and shaken at room temperature, and time-dependent removal of the PAHs by the membrane was monitored. The removal efficiency (%) of the PAHs and heavy metals by the membrane was determined using the following equation

$$\text{Removal efficiency}\ (\%) = (c_0 - c_t)/c_0 \times 100 \quad (1)$$

where c_0 and c_t are the initial and residual concentrations of the PAHs (or heavy metals) in the stock solution and filtrate, respectively. The sorption capacity (q_e) of the membrane was explored for the PAH concentrations of 200, 400, and 600 μg/L, whereas heavy metals with concentrations of 1, 5, 10, and 50 mg/L were used, and q_e values were determined with the following formula

$$q_e(\text{mg/g}) = (c_0 - c_e) \times (V/w) \quad (2)$$

where c_0 and c_e are the initial and equilibrium concentrations of the PAHs (or heavy metals) in the test solution (mg/L), V is the volume of the testing solution in L, and w is the membrane weight in g.

The pseudo first-order and pseudo-second-order kinetics models are used to explore the kinetics behavior of the sorption as given in eqs 3 and 4, respectively.

$$\log(q_e - q_t) = \log q_e - k_1 t/2.303 \quad (3)$$

$$t/q_t = 1/k_2 qe^2 + t/q_e \quad (4)$$

where q_t and q_e (mg/g) are the sorption capacity at time t and equilibrium, respectively. The pseudo-first-order model rate constant k_1 (min^{-1}) and pseudo-second-order kinetics k_2 (g/mg min) were calculated from the equations.

For reusability test, the PAH-treated poly-CD membrane (5 mg) was washed with acetonitrile to remove the adsorbed PAHs from the membrane. Then, the membrane was reused for the sorption experiments. After the sorption tests, the fiber morphology was explored by SEM. On the other hand, the membrane was washed with 2% (v/v) nitric acid solution for the removal of the adsorbed metal ions. Afterward, the same membrane was immersed in fresh metal ion solutions (5 μg/L to 5 mL) to reveal the reusability of poly-CD nanofibers. In addition, the leached amount of metal ions (μg/L) was also detected. Each experiment was repeated three times. The ICP-MS technique was used to examine the results of metal ion removal experiments. After batch adsorption studies, the morphology of the poly-CD membrane was explored by SEM analysis.

4.6. Filtration Test of the Poly-CD Membrane. A dead-end filtration system was used to explore the filtration performance of the membrane using a high-pressure cell (Sterlitech HP4750, Sterlitech Corporation, Kent, WA). The HP4750 system has a volume of 300 mL and is pressurized with nitrogen. The cell possesses an active membrane area of 14.6 cm^2. A pressure gauge and regulator were used to tune the purge pressure in the cell. The rounded membrane with a diameter of 5 cm put in the cell. Prior to the filtration tests, the membrane was conditioned and pressurized with distilled water at 10^4 Pa pressure to able get accurate results. Thereafter, the PAH or metal ion solution (50 mL) transferred into the cell, and the cell pressure kept at 10^4 Pa and the temperature of 25 °C during the filtration. Aqueous PAH solutions (400 and 600 μg/L) or metal solutions (10 and 50 mg/L) were used in the experiments. The filtered solutions were collected into beakers. The experiments were carried out in triplicate, and the mean values were reported with standard deviations. Here, flux (F) and water permeability (P_w) values were also calculated for the poly-CD nanofibers. The F and P_w values of the membranes were calculated using eqs 5 and 6, respectively.

$$F\ (\text{L m}^{-2}\,\text{h}^{-1}) = V\ (\text{L})/A\ (\text{m}^2) \times \Delta t\ (\text{h}) \quad (5)$$

$$P_w\ (\text{L m}^{-2}\,\text{h}^{-1}\,\text{kPa}^{-1}) = F/P_0\ (\text{kPa}) \quad (6)$$

where V is the volume of the permeate used, A is the active membrane area, Δt is the time of permeate collection, and P_0 denotes the applied pressure. The morphology of the nanofibers in the membrane was explored by SEM after the filtration tests.

■ ASSOCIATED CONTENT

Supporting Information

The Supporting Information is available free of charge on the ACS Publications website at DOI: 10.1021/acsomega.9b00279.

Experimental details for XPS and XRD measurements, deconvoluted C1s XPS spectra of the mats, high-resolution XPS spectra of the heavy metals adsorbed on the poly-CD membrane, XRD patterns of HP-β-CD powder and poly-CD membrane, and adsorption of PAHs by glass containers (PDF)

■ AUTHOR INFORMATION

Corresponding Author

*E-mail: tu46@cornell.edu.

ORCID

Fuat Topuz: 0000-0002-9011-4495

Tamer Uyar: 0000-0002-3989-4481

Author Contributions

A.C. and F.T. equally contributed to the manuscript. The manuscript was written through contributions of all authors. All authors have given approval to the final version of the manuscript.

DOI: 10.1021/acsomega.9b00279
ACS Omega 2019, 4, 7850−7860

Funding

The Scientific and Technological Research Council of Turkey (TUBITAK, project# 113Y348) is acknowledged for funding the research.

Notes

The authors declare no competing financial interest.

REFERENCES

(1) Reemtsma, T.; Weiss, S.; Mueller, J.; Petrovic, M.; González, S.; Barcelo, D.; Ventura, F.; Knepper, T. P. Polar Pollutants Entry into the Water Cycle by Municipal Wastewater: A European Perspective. *Environ. Sci. Technol.* **2006**, *40*, 5451−5458.

(2) Sonune, A.; Ghate, R. Developments in wastewater treatment methods. *Desalination* **2004**, *167*, 55−63.

(3) Sánchez-Avila, J.; Bonet, J.; Velasco, G.; Lacorte, S. Determination and occurrence of phthalates, alkylphenols, bisphenol A, PBDEs, PCBs and PAHs in an industrial sewage grid discharging to a Municipal Wastewater Treatment Plant. *Sci. Total Environ.* **2009**, *407*, 4157−4167.

(4) Behera, B. K.; Das, A.; Sarkar, D. J.; Weerathunge, P.; Parida, P. K.; Das, B. K.; Thavamani, P.; Ramanathan, R.; Bansal, V. Polycyclic aromatic hydrocarbons (PAHs) in inland aquatic ecosystems: Perils and remedies through biosensors and bioremediation. *Environ. Pollut.* **2018**, *241*, 212−233.

(5) Tsibart, A. S.; Gennadiev, A. N. Polycyclic aromatic hydrocarbons in soils: Sources, behavior, and indication significance (a review). *Eurasian Soil Sci.* **2013**, *46*, 728−741.

(6) Wilson, S. C.; Jones, K. C. Bioremediation of soil contaminated with polynuclear aromatic hydrocarbons (PAHs): A review. *Environ. Pollut.* **1993**, *81*, 229−249.

(7) Sun, C.; Zhang, J.; Ma, Q.; Chen, Y.; Ju, H. Polycyclic aromatic hydrocarbons (PAHs) in water and sediment from a river basin: sediment-water partitioning, source identification and environmental health risk assessment. *Environ. Geochem. Health* **2017**, *39*, 63−74.

(8) Nwaichi, E. O.; Ntorgbo, S. A. Assessment of PAHs levels in some fish and seafood from different coastal waters in the Niger Delta. *Toxicol. Rep.* **2016**, *3*, 167−172.

(9) Shimada, T.; Fujii-Kuriyama, Y. Metabolic activation of polycyclic aromatic hydrocarbons to carcinogens by cytochromes P450 1A1 and1B1. *Cancer Sci.* **2004**, *95*, 1−6.

(10) Plant, A. L.; Knapp, R. D.; Smith, L. C. Mechanism and rate of permeation of cells by polycyclic aromatic hydrocarbons. *J Biol Chem* **1987**, *262*, 2514−2519.

(11) Pratt, M. M.; John, K.; MacLean, A. B.; Afework, S.; Phillips, D. H.; Poirier, M. C. Polycyclic aromatic hydrocarbon (PAH) exposure and DNA adduct semi-quantitation in archived human tissues. *Int. J. Environ. Res. Public Health* **2011**, *8*, 2675−2691.

(12) Mastral, A. M.; Callén, M. S. A review on polycyclic aromatic hydrocarbon (PAH) emissions from energy generation. *Environ. Sci. Technol.* **2000**, *34*, 3051−3057.

(13) *Agency for Toxic Substances and Disease Registry (ATSDR) Case Studies in Environmental Medicine Toxicity of Polycyclic Aromatic Hydrocarbons (PAHs)*; U.S. Environmental Protection Agency (EPA): U.S., 2009; pp 1−68.

(14) Waalkes, M. Cadmium carcinogenesis. *Mutat. Res., Fundam. Mol. Mech. Mutagen.* **2003**, *533*, 107−120.

(15) Järup, L. Hazards of heavy metal contamination. *Br. Med. Bull.* **2003**, *68*, 167−182.

(16) Jaishankar, M.; Tseten, T.; Anbalagan, N.; Mathew, B. B.; Beeregowda, K. N. Toxicity, mechanism and health effects of some heavy metals. *Interdiscip. Toxicol.* **2014**, *7*, 60−72.

(17) Sanders, T.; Liu, Y.; Buchner, V.; Tchounwou, P. B. Neurotoxic effects and biomarkers of lead exposure: a review. *Rev. Environ. Health* **2009**, *24*, 15−45.

(18) Denkhaus, E.; Salnikow, K. Nickel essentiality, toxicity, and carcinogenicity. *Crit. Rev. Oncol. Hematol.* **2002**, *42*, 35−56.

(19) Ishmael, J.; Gopinath, C.; Howell, J. M. Experimental Chronic Copper Toxicity in Sheep. *Res. Vet. Sci.* **1971**, *12*, 358−368.

(20) Fosmire, G. J. Zinc toxicity. *Am. J. Clin. Nutr.* **1990**, *51*, 225−227.

(21) Crossgrove, J.; Zheng, W. Manganese toxicity upon overexposure. *NMR Biomed.* **2004**, *17*, 544−553.

(22) Eeshwarasinghe, D.; Loganathan, P.; Kalaruban, M.; Sounthararajah, D. P.; Kandasamy, J.; Vigneswaran, S. Removing polycyclic aromatic hydrocarbons from water using granular activated carbon: kinetic and equilibrium adsorption studies. *Environ. Sci. Pollut. Res.* **2018**, *25*, 13511−13524.

(23) Topuz, F.; Singh, S.; Albrecht, K.; Möller, M.; Groll, J. DNA nanogels to snare carcinogens: a bioinspired generic approach with high efficiency. *Angew. Chem., Int. Ed.* **2016**, *55*, 12210−12213.

(24) Brandl, F.; Bertrand, N.; Lima, E. M.; Langer, R. Nanoparticles with photoinduced precipitation for the extraction of pollutants from water and soil. *Nat. Commun.* **2015**, *6*, 7765.

(25) Barnes, J. C.; Juríček, M.; Strutt, N. L.; Frasconi, M.; Sampath, S.; Giesener, M. A.; McGrier, P. L.; Bruns, C. J.; Stern, C. L.; Sarjeant, A. A.; Stoddart, J. F. ExBox: a polycyclic aromatic hydrocarbon scavenger. *J. Am. Chem. Soc.* **2013**, *135*, 183−192.

(26) Topuz, F.; Uyar, T. Poly-cyclodextrin cryogels with aligned porous structure for removal of polycyclic aromatic hydrocarbons (PAHs) from water. *J. Hazard. Mater.* **2017**, *335*, 108−116.

(27) Topuz, F.; Uyar, T. Cyclodextrin-functionalized mesostructured silica nanoparticles for removal of polycyclic aromatic hydrocarbons. *J. Colloid Interface Sci.* **2017**, *497*, 233−241.

(28) Alsbaiee, A.; Smith, B. J.; Xiao, L.; Ling, Y.; Helbling, D. E.; Dichtel, W. R. Rapid removal of organic micropollutants from water by a porous β-cyclodextrin polymer. *Nature* **2016**, *529*, 190.

(29) Wei, X.; Sugumaran, P. J.; Peng, E.; Liu, X. L.; Ding, J. Low-Field Dynamic Magnetic Separation by Self-Fabricated Magnetic Meshes for Efficient Heavy Metal Removal. *ACS Appl. Mater. Interfaces* **2017**, *9*, 36772−36782.

(30) Zhao, G.; Li, J.; Ren, X.; Chen, C.; Wang, X. Few-layered graphene oxide nanosheets as superior sorbents for heavy metal ion pollution management. *Environ. Sci. Technol.* **2011**, *45*, 10454−10462.

(31) Gholami Derami, H.; Jiang, Q.; Ghim, D.; Cao, S.; Chandar, Y. J.; Morrissey, J. J.; Jun, Y.-S.; Singamaneni, S. A robust and scalable polydopamine/bacterial nanocellulose hybrid membrane for efficient wastewater treatment. *ACS Appl. Nano Mater.* **2019**, *2*, 1092−1101.

(32) Sun, H.; Jiang, J.; Xiao, Y.; Du, J. Efficient Removal of Polycyclic Aromatic Hydrocarbons, Dyes, and Heavy Metal Ions by a Homopolymer Vesicle. *ACS Appl. Mater. Interfaces* **2018**, *10* (1), 713−722.

(33) Morin-Crini, N.; Winterton, P.; Fourmentin, S.; Wilson, L. D.; Fenyvesi, É.; Crini, G. Water-insoluble β-cyclodextrin−epichlorohydrin polymers for removal of pollutants from aqueous solutions by sorption processes using batch studies: A review of inclusion mechanisms. *Prog. Polym. Sci.* **2018**, *78*, 1−23.

(34) Nagy, Z. M.; Molnár, M.; Fekete-Kertész, I.; Molnár-Perl, I.; Fenyvesi, É.; Gruiz, K. Removal of emerging micropollutants from water using cyclodextrin. *Sci. Total Environ.* **2014**, *485−486*, 711−719.

(35) Crini, G.; Fourmentin, S.; Fenyvesi, É.; Torri, G.; Fourmentin, M.; Morin-Crini, N. Cyclodextrins, from molecules to applications. *Environ. Chem. Lett.* **2018**, *16*, 1361−1375.

(36) Shabtai, I. A.; Mishael, Y. G. Polycyclodextrin-Clay Composites: Regenerable Dual-Site Sorbents for Bisphenol A Removal from Treated Wastewater. *ACS Appl. Mater. Interfaces* **2018**, *10*, 27088−27097.

(37) Crini, G.; Exposito Saintemarie, A.; Rocchi, S.; Fourmentin, M.; Jeanvoine, A.; Millon, L.; Morin-Crini, N. Simultaneous removal of five triazole fungicides from synthetic solutions on activated carbons and cyclodextrin-based adsorbents. *Heliyon* **2017**, *3*, No. e00380.

(38) Euvrard, É.; Morin-Crini, N.; Druart, C.; Bugnet, J.; Martel, B.; Cosentino, C.; Moutarlier, V.; Crini, G. Cross-linked cyclodextrin-based material for treatment of metals and organic substances present in industrial discharge waters. *Beilstein J. Org. Chem.* **2016**, *12*, 1826−1838.

(39) Sherje, A. P.; Dravyakar, B. R.; Kadam, D.; Jadhav, M. Cyclodextrin-based nanosponges: A critical review. *Carbohydr. Polym.* **2017**, *173*, 37−49.

DOI: 10.1021/acsomega.9b00279
ACS Omega 2019, 4, 7850−7860

(40) Celebioglu, A.; Demirci, S.; Uyar, T. Cyclodextrin-grafted electrospun cellulose acetate nanofibers via ″Click″ reaction for removal of phenanthrene. *Appl. Surf. Sci.* **2014**, *305*, 581−588.
(41) Kayaci, F.; Aytac, Z.; Uyar, T. Surface modification of electrospun polyester nanofibers with cyclodextrin polymer for the removal of phenanthrene from aqueous solution. *J. Hazard. Mater.* **2013**, *261*, 286−294.
(42) Celebioglu, A.; Yildiz, Z. I.; Uyar, T. Electrospun crosslinked poly-cyclodextrin nanofibers: Highly efficient molecular filtration thru host-guest inclusion complexation. *Sci. Rep.* **2017**, *7*, 7369.
(43) Celebioglu, A.; Topuz, F.; Uyar, T. Water-insoluble hydrophilic electrospun fibrous mat of cyclodextrin-epichlorohydrin polymer as highly effective sorbent. *ACS Appl. Polym. Mater.* **2019**, *1*, 54−62.
(44) Ducoroy, L.; Bacquet, M.; Martel, B.; Morcellet, M. Removal of heavy metals from aqueous media by cation exchange nonwoven PET coated with β-cyclodextrin-polycarboxylic moieties. *React. Funct. Polym.* **2008**, *68*, 594−600.
(45) Morillo, E.; Sánchez-Trujillo, M. A.; Moyano, J. R.; Villaverde, J.; Gómez-Pantoja, M. E.; Pérez-Martínez, J. I. Enhanced solubilisation of six PAHs by three synthetic cyclodextrins for remediation applications: molecular modelling of the inclusion complexes. *PLoS One* **2012**, *7*, No. e44137.
(46) Immel, S.; Lichtenthaler, F. W. Per-O-methylated α- and β-CD: Cyclodextrins with Inverse Hydrophobicity. *Starch Staerke* **1996**, *48*, 225−232.
(47) He, X.; Wu, Z.; Sun, Z.; Wei, X.; Wu, Z.; Ge, X.; Cravotto, G. A novel hybrid of β-cyclodextrin grafted onto activated carbon for rapid adsorption of naphthalene from aqueous solution. *J. Mol. Liq.* **2018**, *255*, 160−167.
(48) Obaid, M.; Ghouri, Z. K.; Fadali, O. A.; Khalil, K. A.; Almajid, A. A.; Barakat, N. A. M. Amorphous SiO2 NP-Incorporated Poly-(vinylidene fluoride) Electrospun Nanofiber Membrane for High Flux Forward Osmosis Desalination. *ACS Appl. Mater. Interfaces* **2016**, *8*, 4561−4574.
(49) Dobosz, K. M.; Kuo-Leblanc, C. A.; Martin, T. J.; Schiffman, J. D. Ultrafiltration membranes enhanced with electrospun nanofibers exhibit improved flux and fouling resistance. *Ind. Eng. Chem. Res.* **2017**, *56*, 5724−5733.
(50) Coelho, D.; Sampaio, A.; Silva, C. J. S. M.; Felgueiras, H. P.; Amorim, M. T. P.; Zille, A. Antibacterial electrospun poly(vinyl alcohol)/enzymatic synthesized poly(catechol) nanofibrous midlayer membrane for ultrafiltration. *ACS Appl. Mater. Interfaces* **2017**, *9*, 33107−33118.
(51) Dong, Z.-Q.; Wang, B.-J.; Ma, X.-h.; Wei, Y.-M.; Xu, Z.-L. FAS Grafted electrospun poly(vinyl alcohol) nanofiber membranes with robust superhydrophobicity for membrane distillation. *ACS Appl. Mater. Interfaces* **2015**, *7*, 22652−22659.
(52) Ma, H.; Burger, C.; Hsiao, B. S.; Chu, B. Nanofibrous microfiltration membrane based on cellulose nanowhiskers. *Biomacromolecules* **2012**, *13*, 180−186.

DOI: 10.1021/acsomega.9b00279
ACS Omega 2019, 4, 7850−7860